

Comparison of MODIS broadband albedo over an agricultural site with ground measurements and values derived from Earth observation data at a range of spatial scales

M. DISNEY^{†*}, P. LEWIS[‡], G. THACKRAH[‡], T. QUAIFFE[†] and M. BARNSELEY[§]

[†]Centre for Terrestrial Carbon Dynamics, Department of Geography, University College London, 26 Bedford Way, London WC1H 0AP, UK

[‡]Department of Geography, University College London, 26 Bedford Way, London WC1H 0AP, UK

[§]EME0 Group, Department of Geography, University of Wales Swansea, Singleton Park, SA2 8PP, UK

(Received 4 August 2003; in final form 22 March 2004)

Abstract. Land surface albedo is dependent on atmospheric state and hence is difficult to validate. Over the UK persistent cloud cover and land cover heterogeneity at moderate (km-scale) spatial resolution can also complicate comparison of field-measured albedo with that derived from instruments such as the Moderate Resolution Imaging Spectrometer (MODIS). A practical method of comparing moderate resolution satellite-derived albedo with ground-based measurements over an agricultural site in the UK is presented. Point measurements of albedo made on the ground are scaled up to the MODIS resolution (1 km) through reflectance data obtained at a range of spatial scales. The point measurements of albedo agreed in magnitude with MODIS values over the test site to within a few per cent, despite problems such as persistent cloud cover and the difficulties of comparing measurements made during different years. Albedo values derived from airborne and field-measured data were generally lower than the corresponding satellite-derived values. This is thought to be due to assumptions made regarding the ratio of direct to diffuse illumination used when calculating albedo from reflectance. Measurements of albedo calculated for specific times fitted closely to the trajectories of temporal albedo derived from both Systeme pour l'Observation de la Terre (SPOT) Vegetation (VGT) and MODIS instruments.

1. Introduction

With the launch of the Moderate Resolution Imaging Spectrometer (MODIS) instrument aboard the NASA Terra platform in December 1999, a new capability for deriving moderate resolution estimates of broadband albedo was initiated (Schaaf *et al.* 2001, 2002). Albedo is defined as the ratio of outgoing to incoming radiation at the Earth's surface. In order to understand and characterize the fluxes of energy at the Earth's surface, albedo must be known as accurately as possible

*Corresponding author; e-mail: mdisney@geog.ucl.ac.uk

(Sellers 1992). It defines the lower boundary condition of the atmosphere and consequently determines how much incoming solar radiation is reflected (in the shortwave part of the spectrum) or absorbed and re-emitted (in the thermal infrared (IR) part of the spectrum) (Dickinson *et al.* 1990, Sellers 1995).

In practice broadband (visible and near-infrared (NIR)) albedo is a difficult property to measure for several reasons. First, albedo is dependent on the surface bidirectional reflectance distribution function (BRDF). BRDF describes the (spectral) surface reflectance at a specific wavelength λ , viewed from position $\mathbf{\Omega}(\theta_v, \phi_v)$ under illumination from a source located in direction $\mathbf{\Omega}'(\theta_i, \phi_i)$, where $\theta_{v,i}$ and $\phi_{v,i}$ are the view zenith and azimuth angles respectively. BRDF is a function of the size and distribution of objects on the surface as well as the spectral reflectance properties of those materials i.e.

$$\text{BRDF}(\mathbf{\Omega}, \mathbf{\Omega}') = \frac{dL_e(\mathbf{\Omega}, \mathbf{\Omega}')}{dE_i(\mathbf{\Omega}')} \text{ (sr}^{-1}\text{)} \quad (1)$$

where dL_e is the incremental radiance reflected from the surface into the differential solid angle in the viewing direction $\mathbf{\Omega}$ ($\text{W m}^{-2} \text{sr}^{-1}$) (Nicodemus *et al.* 1977, Martonchik *et al.* 1998); dE_i is the incremental irradiance ($\text{W m}^{-2} \text{sr}^{-1}$) arriving from the illumination direction, $\mathbf{\Omega}'$ i.e. $dE_i = L_i(\mathbf{\Omega}') \cos \theta_i \sin \phi_i d\theta_i d\phi_i$.

In addition to the dependence on surface reflectance (an intrinsic surface property), albedo is dependent on the proportions of direct and diffuse radiation arriving at the surface, which are a function of atmospheric state (scattering behaviour and optical depth) and sun position. This dependence of albedo on atmospheric state means it is not an intrinsic property of the surface (unlike BRDF) but can change with changing atmosphere. Liang and Lewis (1996) have shown that narrowband (spectral) albedo can be approximated as the sum of the albedo resulting from the diffuse component of atmospheric scattering, D , and the albedo resulting from the direct component, $1-D$ i.e.

$$\alpha(\lambda) = (1 - D(\lambda, \mathbf{\Omega}', \tau)) \bar{\rho}(\lambda, \mathbf{\Omega}') + D(\lambda, \mathbf{\Omega}', \tau) \bar{\bar{\rho}}(\lambda) \quad (2)$$

where $\bar{\rho}$ is the surface directional hemispherical reflectance i.e. BRDF resulting from a purely directional illumination source integrated over the entire viewing hemisphere (or, conversely, the directional reflectance resulting from a purely hemispherical (diffuse) illumination source); $\bar{\bar{\rho}}$ is the bi-hemispherical reflectance i.e. $\bar{\rho}$ integrated over the illumination (or viewing) hemisphere; τ is the atmospheric optical depth.

In addition to surface reflectance and atmospheric state, broadband albedo depends on the relative weighting of energy arriving across the solar spectrum, not just at a specific wavelength (Brest and Goward 1987, Lewis *et al.* 1999, Song and Gao 1999). Most remote sensing instruments measure surface reflectance across fixed width spectral bands at certain points in the spectrum (visible and near IR for example). Estimating broadband albedo therefore also requires some way of interpolating/extrapolating a limited number of spectral estimates of albedo across the spectrum. This requires knowledge of the spectral distribution of incoming solar radiation (both direct and diffuse) (Brest and Goward 1987). In practice this can be done using a weighted summation of spectral terms i.e.

$$\alpha = \int_{SW} p(\lambda) \alpha(\lambda) d\lambda \quad (3)$$

where $p(\lambda)$ is the proportion of illumination in the solar spectrum at wavelength λ .

Recently however, Liang (2000) and Liang *et al.* (2002, 2003) have conducted a series of radiative transfer model simulations under varying atmospheric and surface conditions to show that it is possible to calculate coefficients for narrow- to broadband albedo conversion for a range of different sensors. These weightings are shown to generate albedo values within 2% of measured values in most cases across the visible, shortwave IR and near IR parts of the spectrum.

The dependence of albedo on BRDF, atmospheric state and spectral weighing makes it difficult to calculate directly. It is also difficult to validate accurately (Disney *et al.* 1997, Lewis *et al.* 1999, Lucht *et al.* 2000, Liang *et al.* 2003). The MODIS BRDF/albedo product (MOD43) is the first operational albedo product produced from spaceborne data, in near real-time (Schaaf *et al.* 2002). The MOD43 product is derived at 1 km spatial resolution in three broadband regions (visible, shortwave-infrared (SWIR), IR) from limited angular samples of spectral reflectance, collected over 8 or 16 day periods, during which surface BRDF is assumed to be (near) invariant. These estimates can be interpolated and/or extrapolated to arbitrary viewing and illumination angles using semi-empirical kernel-driven models of BRDF (Wanner *et al.* 1997, Lucht *et al.* 1999). The kernel-driven approach permits simple calculation of directional hemispherical reflectance $\bar{\rho}$, by integrating the angular kernels over the viewing (or illumination) hemisphere. $\bar{\rho}$ is often termed 'black-sky' albedo i.e. albedo for a perfectly direct illumination source (no diffuse component). Estimates of bihemispherical reflectance, $\bar{\rho}$, are produced by integrating $\bar{\rho}$ over the illumination (or viewing) hemisphere. $\bar{\rho}$ is often termed 'white-sky' albedo i.e. albedo under perfectly diffuse illumination (no direct component). Spectral albedo is then calculated as a weighted sum of black and white-sky albedo, where the weights are determined by the ratio of direct to diffuse illumination as in equation (2). This is the basis of the MOD43 BRDF/albedo product (Strahler *et al.* 1999).

The need to derive and validate broadband albedo has led to a number of validation efforts over a range of land cover types (Lucht *et al.* 2000, Liang *et al.* 2003). This paper presents comparisons of BRDF/albedo calculated over an agricultural field site in order to provide a consistency check on the MOD43 albedo product and associated parameters. This is part of validation work for the MODIS products that is ongoing worldwide at selected core validation sites (Morissette *et al.* 2002).

This paper presents a comparison of broadband albedo values derived from six different sources, at a range of spatial scales:

1. Point measurements of albedo made in the field;
2. Albedo derived from field-measured reflectance data;
3. Albedo derived from airborne (HyMAP) reflectance data;
4. Albedo derived from high resolution spaceborne (Landsat Thematic Mapper) data;
5. Albedo derived from moderate resolution spaceborne (Système pour l'Observation de la Terre Vegetation) data;
6. MOD43 albedo product derived from MODIS reflectance data.

As noted above, albedo is both difficult to measure and validate for a variety of reasons. It is not possible to measure albedo directly at 500 m scale, let alone 1 km, unless severe assumptions about surface reflectance homogeneity are made. Such assumptions are not necessarily valid for the atmosphere above the surface at these scales anyway, particularly in the UK. As a result, the type of multi-scale comparison presented here is the only way in which a moderate resolution product

such as MOD43 can be checked for consistency over time, and confidence in its accuracy be established. Although MODIS products are produced continuously, it is both expensive and difficult practically to obtain airborne and/or high resolution spaceborne data for anything other than a few dates. As a result, comparison of MODIS albedo will typically be made at one or two points in time. This is particularly true of sites in the UK where cloud cover tends to severely reduce temporal coverage even during summer months.

The purpose of this study is to provide a consistency check of the MODIS MOD43 BRDF/albedo product using BRDF and albedo values derived from field measurements, airborne data and other, higher spatial resolution satellite data. Intercomparisons of BRDF model parameters derived using these at different angular sampling configurations and base spatial resolutions are presented.

2. Method

The field site used in this study is Hill Farm, Barton Bendish, Norfolk, UK (52.62°N 0.54°E), owned and operated by Albanwise UK, Ltd King's Lynn, Norfolk, UK, which is a MODIS core validation site. The Barton Bendish area is typical of the intensive agricultural activity in this region of the UK, comprising cereal crops (winter/spring wheat, barley, corn/maize), legumes (peas, beans), potatoes and sugar beet. Figure 1 shows the Barton Bendish area highlighted in a composite of HyMAP (Hyperspectral Mapper) flightlines (described below). The Hill Farm area is outlined; RAF Marham air base can be seen at the top of the HyMAP image. At the time of this image acquisition (17 June 2000) the wheat fields had Leaf Area Index (LAI) values of 3.8–5, corresponding to canopy cover of 85–95% (Shaw 2002).

The region is low-lying (a few metres above sea level), flat and has field sizes of the order of a few tens of hectares. This is relatively large by UK standards but extremely heterogeneous in comparison with other MODIS core validation sites in the US and Russia. This implies that any assumption of homogeneity at the scale of the MOD43 product (1 km) is not likely to be valid. For this reason comparison of MOD43 BRDF/albedo with field measurements is only possible by scaling up from the point/field level, through high resolution airborne and satellite data, in order that spatial consistency can be checked at each scale.

Table 1 contains a summary of the various datasets that are used in this study, the dates on which they were collected and the various characteristics of these data. The collection and processing of these data are described below.

2.1. Field-measured albedo

Measurements of broadband albedo were made in three wheat fields characteristic of the site as a whole (marked on figure 1) using a Kipp and Zonen CNR 1 net radiometer instrument mounted on a tripod 3.5 m above ground level. The distance to the top of the canopy from the CNR 1 instrument ranged from 3.5 m for bare soil to 2.5 m for mature wheat (Shaw 2002). The CNR 1 instrument was placed in areas of uninterrupted homogeneous cover as far as possible from paths and field boundaries. The net radiometer consists of two pyranometers to provide net solar radiation in the range 0.3–3 μm (180° upward FOV, 150° downward FOV) and two pyrgeometers to record net longwave radiation in the range 3–50 μm . Addition of the solar and longwave quantities gives net radiation.



Figure 1. Six flightlines of HyMAP data over the Barton Bendish site collected as part of the SHAC campaign (Saich *et al.* 2001) on 17 June 2000. Hill Farm is outlined as are the wheat fields used for point measurement of albedo (dotted outlines).

Albedo measured using the CNR 1 is nominally a point measurement but, as the instrument has a (downward looking) 150° FOV, recorded albedo values will correspond to radiation reflected from a region surrounding the instrument to a radius of between 9.3 and 13 m (depending on canopy height as above). Albedo typically starts and ends the day higher in value than at solar noon (caused by an increased proportion of diffuse irradiance resulting from increased scattering over the longer path length at high sun zenith angles), but the total downwelling radiation is of course much higher at solar noon and hence more important in terms of total energy available to be absorbed or reflected. The values of albedo

Table 1. Summary of the various data used in this study, the dates on which they were collected and the various characteristics of these data.

| Sensor | Measurement type | Date | Spatial resolution | Spectral resolution (μm) | Angular sampling |
|--|---|---|--------------------|---------------------------------------|--|
| CNR 1 net radiometer (net solar radiation) | Broadband hourly albedo | 2, 4, 5, 6, 8 May 2000 17–22 June 2000 | Point sample | 0.3–3 and 3–50 | Hemispherical |
| ASD spectro-radiometer | Spectral reflectance | 7 and 9 May 2000, 17 June 2000 | Few cm | 0.3–2.5 in steps of 1 nm | IFOV of 8° , measurements made at nadir and one or two angles off nadir $\pm 34^\circ$ view zenith variation within each flightline |
| HyMAP | Airborne hyperspectral reflectance | 17 June 2000 | 4.4 m | 0.437–2.485 in steps of ~ 16 nm. | Very little (single image) |
| Landsat TM | Spaceborne multispectral reflectance | 11 July 1999 | 30 m | 0.45–2.35 in six broad bands | N/A |
| SPOT-VGT | Albedo derived from BRDF | 17 May 1999 to 1 October 1999 | 1 km | 0.43–1.75 in four broad bands | N/A |
| MODIS | MOD43 spaceborne BRDF/albedo (Terra only) | 1 October 2000 to 1 October 2002 | 500 m, 1 km | Broadband (0.3–5) | N/A |

closest in time of day to those of the satellite and airborne measurements are used here. Measured albedo was convolved with the instrument spectral response function specified by the manufacturer (<http://www.kippzonen.com/>).

2.2. Field-measured reflectance

Reflectance of winter wheat was measured in several fields using an ASD FieldSpec Pro spectroradiometer (http://www.asdi.com/asdi_t2_pr_sp_fsp.html) held at 1 m above the level of the canopy top (Shaw 2002). Reflectance was measured at 30 m intervals along a transect diagonal to the row direction within each field in order to characterize within-field variability which can arise as a result of variable soil quality and uneven irrigation and application of fertiliser (Disney 2002). The ASD instrument averages several spectra obtained over a period of a few seconds at each point. This acts to increase the effective instrument integration time and provides improved signal-to-noise ratio (SNR). Reflectance was sampled at between 15 and 20 points along each transect (depending on field size) and samples were averaged to provide per-field estimates of reflectance. An 8° FOV fore-optic was used on the radiometer resulting in a projected FOV on the ground of radius 0.2 m. Reflectance was measured at nadir and 30° either side of nadir in the solar principle plane in order to characterize the directionality of the canopy reflectance. The spectral range of the instrument is 350 to 2500 nm in 1.5 nm steps, but only data in the range 450 to 2450 nm were used to avoid the lower signal-to-noise at the extremes. Examples of spectra measured within winter wheat fields are shown in figure 2 for dates in May and June 2000.

It can be seen that the field-measured spectra in figure 2 are characteristic of photosynthetically active (green) vegetation. There is little variation in the visible chlorophyll absorption region between the different days and times, but some in the NIR. In particular, reflectance increases significantly from DOY (day-of-year) 126 and 129 to DOY 168. This is to be expected as the crop has developed significantly

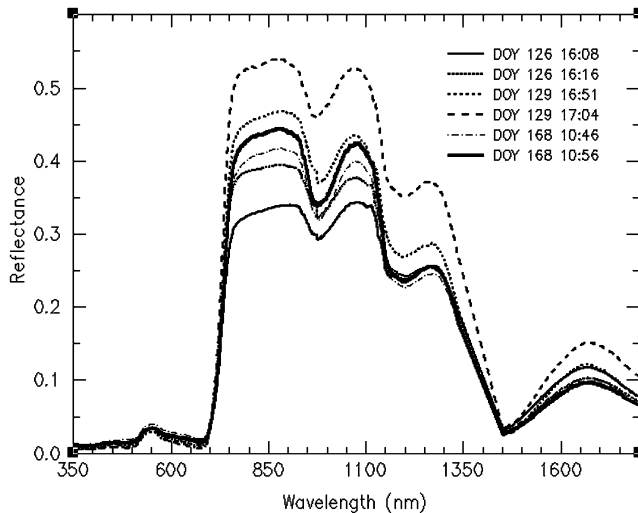


Figure 2. Reflectance spectra measured within winter wheat fields using an ASD FieldSpec Pro spectroradiometer for three dates: DOY (day-of-year) 126 and 129 (6 and 9 May 2000); DOY 168 (17 June 2000).

during this time and is now close to maturity. It should be noted that there is a discontinuity in the measured spectra between 1300 nm and 1450 nm due to a change in the detector semiconductor composition: data in this range are excluded here. Variation in reflectance with view zenith angle on a given date was far less than that due to the differences in dates seen in figure 2. There is little or no variation at visible wavelengths, while at view zenith angles of 30° an increase in reflectance of a few per cent is seen. For calculation of albedo the field-measured reflectance of wheat is assumed to be Lambertian i.e. directionally invariant. This is a reasonable assumption given the lack of observed directional variation.

In order to calculate broadband albedo from field-measured reflectance, the spectral reflectance is first converted to spectral albedo. In order to do this, observed $\bar{\rho}$ (assuming Lambertian wheat reflectance) were weighted according to the spectral distribution incoming solar irradiance at the time of measurement, as in equation (2). The incoming solar irradiance at ground level was calculated using the geometrical, spectral sky radiance distribution model of Zibordi and Voss (1989). This model allows calculation of the total diffuse component of sky radiance, D (the direct component is then $1-D$). Sky radiance was calculated for the same time of day as the reflectance measurements were taken, assuming a continental aerosol model and a mid-latitude summer atmospheric profile. The resulting sky radiance distribution was then used to weight the spectral estimates of reflectance to yield narrowband (spectral) albedo. This was converted to broadband albedo by performing a spectral integral of the form described in equation (3).

2.3. HyMAP airborne data

Airborne data over the Barton Bendish site were collected as part of the SHAC (SAR and Hyperspectral Airborne Campaign) experiment in 2000 (Saich *et al.* 2001). The instrument used is the HyMAP whiskbroom digital scanner, a multispectral scanner with 128 channels from the visible to the NIR (400–2500 nm). For the SHAC campaign HyMAP was operated using 126 bands from 437 nm to 2485.9 nm in steps of 16 nm. Six flightlines were flown on 17 June 2000 between 11:15 and 11:56. The flightlines were flown on headings as close to 180° and 0° as possible, at an altitude of 2100 m above ground level. The solar azimuth angles range from 160° for the 11:15 flightline to 179° for the 11:56 flightline. The solar zenith angle varies only 1.5° during this period, from 30.5° to 29°. The flightline directions thus vary from 20° off the solar principal plane at 11:15 to almost directly in the solar principal plane at 11:56. This is intended to maximize the observed directional signal as far as possible, which tends to be at its greatest in the solar principal plane.

There is some overlap between flightlines (HyMAP has a FOV of around 60°) so some multiangular sampling is achieved, but this is very limited. This is illustrated in figure 1. The overlap can be inferred from the lateral boundaries of each strip. Hill Farm appears in the central three flightlines only, and of the three wheat fields marked in figure 1, only two view zenith samples are obtained. The SHAC HyMAP data were geometrically corrected and registered to OSGB36. Atmospheric correction was carried out using the ATREM model (Gao *et al.* 1996), a radiative transfer model based on the 6S model of Vermote *et al.* (1997). Atmospherically corrected HyMAP reflectance spectra were 'polished' to remove spectral artifacts (due to wavelength registration errors and molecular absorption residuals) using the EFFORT model of Boardman (1998). For atmospheric

correction a continental aerosol model and mid-latitude summer atmospheric profile were assumed. HyMAP spectra derived from mean wheat field reflectance for selected angular bins are shown in figure 3.

Figure 3 shows three spectra from three separate view zenith angles including nadir. The lack of observed variation with view angle in the visible and IR is apparent. However, the spectra obtained at the larger view zenith angles (18 and 26°) are a few per cent higher in the SWIR than in the visible. This is consistent with the angular signature of vegetation reflectance, which typically displays increasing reflectance with view zenith away from nadir. This is a result of increased volume scattering caused by the longer (viewing) path length through the canopy at higher view zenith angles.

There is a discontinuity in the observed HyMAP spectra 3 between 1800 and 1950 nm due to detector behaviour. The field-measured spectra and the HyMAP spectra shown in figures 2 and 3 respectively agree well in general. However the field-measured spectra for DOY 168 (the date of the HyMAP overpass) are slightly higher in the visible part of the spectrum and slightly lower in the NIR. It should be noted that the spectra in figure 3 incorporate some spatial variation due to the intra-field variability of the wheat crops (Disney 2002). The general agreement between the field-measured and HyMAP spectra provides some independent confirmation of consistency between the observations (and gives some confidence in the atmospheric correction used to convert HyMAP observed radiance to at-ground reflectance, a potential source of error).

With so little view and sun zenith angle variation and sparse angular sampling it is not feasible to follow the standard path of inverting a model of BRDF against observed directional reflectance and using the resultant parameters to calculate $\bar{\rho}$, $\bar{\rho}$ and from this, albedo. In this case, HyMAP reflectance of all the known fields of wheat within the Hill Farm area (not just the three noted in figure 1) were spatially aggregated to produce a mean wheat reflectance, with correspondingly aggregated viewing and illumination angles (assuming the various wheat fields are broadly homogeneous). This is illustrated in figure 4 which shows HyMAP reflectance at

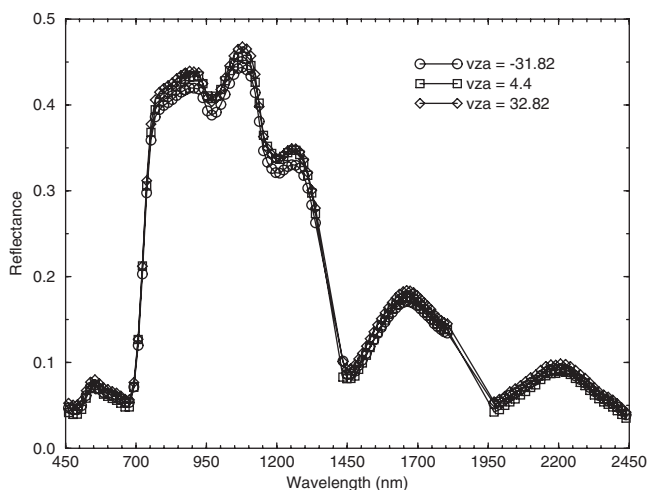


Figure 3. HyMAP spectra derived from mean wheat field reflectance for angular bins of 18°, 26° and -4°, where positive (negative) angles indicate the forward (back-scattering) direction.

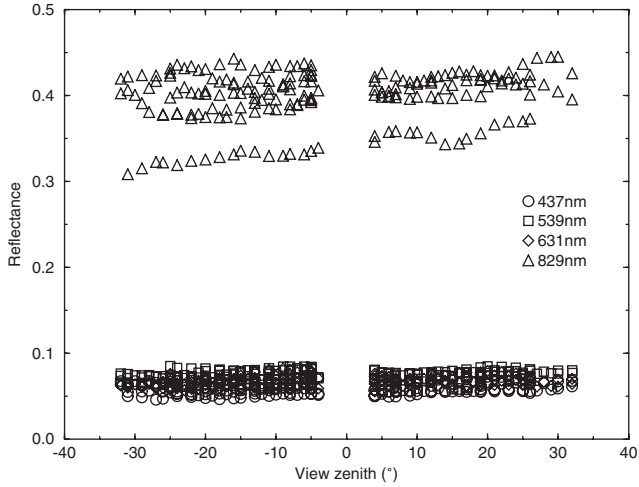


Figure4. HyMAP reflectance at four wavebands (three visible, plus SWIR) at all available viewing zenith angles for the six separate HyMAP flightlines.

four wavebands (visible blue, green, red and NIR) at all available viewing zenith angles for the six separate HyMAP flightlines.

It can be seen that there is very little variation in magnitude with viewing angle in the visible (1 or 2%) but up to around 10% in the NIR. As a result of this lack of observed angular variation in mean wheat reflectance, the various values for each viewing angle were aggregated into a mean 'scene' wheat reflectance. This is shown in figure 5 for the same wavebands.

The lack of sufficient angular sampling of wheat reflectance for BRDF model inversion necessitated the assumption of Lambertian reflectance of the wheat fields in order to calculate $\bar{\rho}$ and then albedo. The lack of angular variation in figures 4 and 5 suggests this assumption is reasonable. The aggregated HyMAP wheat reflectance observations were weighted by incoming spectral irradiance calculated

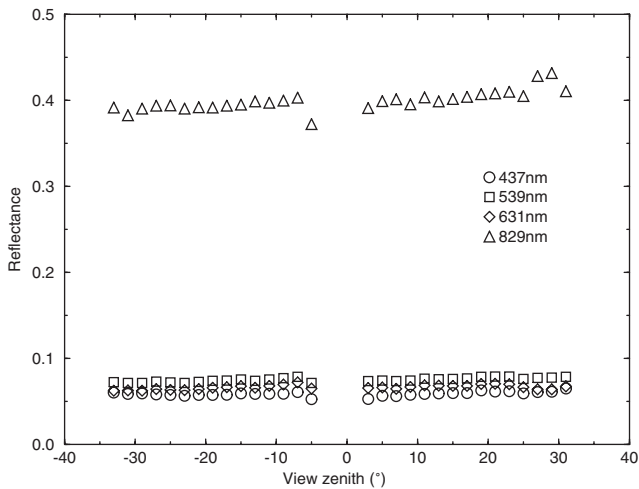


Figure 5. Aggregated 'scene' wheat reflectance at four wavebands (three visible, plus SWIR) generated from the HyMAP data shown in figure 5.

using the Zibordi-Voss model as described above for the field-measured reflectance data. This resulted in values of narrowband (spectral) albedo. These values were converted to broadband albedo by integrating across the solar spectrum, also as above.

2.4. Landsat Thematic Mapper (TM) data

A Landsat TM image over the study area was obtained for 11 July 1999 (i.e. 11 months prior to the HyMAP flights). No Landsat TM data were available for the same time period in 2000 due to lack of suitable cloud-free conditions. However, the distribution of crops planted at Hill Farm during 1999 was identical to that during 2000 therefore the spatial heterogeneity should be very similar in 1999 to 2000. It is also true to say that the least variation in crop reflectance occurs between late June and late July i.e. after the crop has reached maturity but prior to harvest in mid-to-late August (Disney 2002). This, along with farm practices which are consistent from year to year, indicate that it is reasonable to assume that the reflectance behaviour observed in the 1999 Landsat TM scene should be broadly consistent with that witnessed at the same time the following year, and for a two-week period either side of the acquisition date (barring some anomalous climatic or agricultural event).

Landsat TM data are 30 m spatial resolution and comprise six wavebands in the visible and NIR part of the spectrum (see table 1). The Landsat TM scene was atmospherically corrected to surface radiance using the 6S atmospheric correction code (Vermote *et al.* 1997) assuming a continental aerosol model, mid-latitude summer atmospheric profile (as for the HyMAP data) and homogeneous surface reflectance of green vegetation. An estimate of atmospheric visibility at ground level was obtained from the UK Meteorological Office station at Santon Downham, Norfolk (15 km from the Barton Bendish site), on the date of image acquisition (data provided by British Atmospheric Data Centre: <http://badc.nerc.ac.uk/home/>). This is used within 6S to estimate aerosol optical thickness.

Once again, the reflectance of the wheat fields was assumed to be Lambertian and estimates of the proportions of direct and diffuse illumination were obtained from the Zibordi-Voss sky radiance model (Zibordi and Voss 1989). Spectral albedo was then calculated as above. In order to calculate broadband albedo, the coefficients of Liang (2000) were used. The broadband albedo at Landsat TM resolution (30 m) were also aggregated to the same 1 km resolution as the MOD43 albedo product. In this way comparisons can be made between data at higher resolution (point-scale albedo, field-measured reflectance, HyMAP data) as well as with the lower resolution data (SPOT-VGT and MOD43).

2.5. SPOT-VGT data

The SPOT-VGT instrument is a wide FOV (swath width of 2250 km) multispectral sensor with a spatial resolution of 1 km and four spectral bands in the visible blue and red, NIR and SWIR (see table 1). Daily top-of-atmosphere data acquired by SPOT-VGT, from 17 May 1999 to 1 October 1999 were obtained. The data are geometrically corrected at the Center pour Traitement Images Vegetation (CTIV) using information from the onboard navigation systems and a global database of ground control points (Passot 2000, Sylvander *et al.* 2000). This achieves a multi-temporal pixel-to-pixel registration of better than half a pixel (<500 m). Atmospheric correction was performed in-house using a specially

adapted version of the Simplified Method for Atmospheric Correction (SMAC) (Rahman and Dedieu 1994). The driving parameters for the atmospheric correction (aerosol optical depth, water vapour density and ozone concentration) were supplied with the SPOT-VGT data.

In the same manner as for production of the MOD43 BRDF/albedo product, linear kernel-driven models of BRDF were inverted against the data to produce model parameter estimates (Strahler *et al.* 1999). The principal difference between the MOD43 BRDF/albedo product being that the SPOT-VGT data used to invert the model were taken from 30 day periods to provide better angular sampling (at the expense of lower sensitivity to surface reflectance dynamics). From the derived BRDF model parameters values of spectral albedo at 1 km resolution were generated. Spectral albedo values were converted to broadband values using the coefficients described by Liang (2000). The pixel centred on Hill Farm within each SPOT-VGT albedo scene was extracted along with the surrounding pixels. This allows consistency of albedo between neighbouring pixels to be examined (we would not expect large variations given the assumption made above that the region is relatively homogeneous at 1 km scale).

2.6. MOD43 data

MOD43 BRDF/albedo data were obtained for the start of October 2000 to the end of September 2002 (from the Terra platform only). These data are 1 km spatial resolution, produced from the MODIS 16-day BRDF product. The BRDF, albedo and nadir surface reflectance of each pixel are modelled at a spatial resolution of 1 km by inverting multirate, multiangular, cloud-free, atmospherically corrected surface reflectance observations acquired by MODIS in a 16-day period (MODIS orbital double repeat cycle). The product is derived in seven spectral bands, as well as across the total shortwave region (0.3–5 μm). It is this latter product that is used here. The retrieved kernel-driven model BRDF model parameters quantify intrinsic surface properties decoupled from the prevailing atmospheric state and hence provide information on the angular variation of surface reflectance (and how it changes with time). It is these model parameters which are used to calculate black-sky and white-sky albedo. The pixels matching the locations of those extracted from the SPOT-VGT data were extracted from the MODIS data, along with pixels surrounding this region to provide a check on consistency.

Following this, the time series of broadband albedo from October 2000 to September 2002 were compared with the time series of SPOT-VGT albedo values covering the period 17 May 1999 to 1 October 1999. Clearly, these are different years but the trends in albedo calculated from both instruments can be compared for temporal consistency (the surface and cover type are not expected to change very much from year to year). Albedo values calculated from the field measurements, HyMAP and Landsat TM data were also compared with the SPOT-VGT and MOD43 time series. The field data were only comparable at a single point in time with the satellite-derived time series (or two points in the case of the field-measured albedo and reflectance). This is the fundamental problem of validating time series data such as these. If the field measurements agree with the HyMAP and Landsat TM measurements, then we can have some confidence the ability of the field measurements to characterize the airborne data. A subsequent comparison of the airborne data with the spaceborne time-series will then indicate

whether the spaceborne data are consistent in magnitude with the airborne and field-measured data.

Comparison can also be made between the three linear kernel-driven BRDF model parameters (isotropic, geometric-optic and volumetric) from year to year in order to check consistency between these values. Inconsistencies in surface reflectance behaviour between the SPOT-VGT and MODIS data, which may not be apparent in the broadband albedo, should be more obvious in the model parameters as these are related to intrinsic surface properties (Wanner *et al.* 1997, Disney 2002). Results of these various comparisons are presented below. However, it should be noted that the majority of MOD43 BRDF model parameter values generated over the Barton Bendish region have been generated via so-called 'magnitude inversions' (Strugnell and Lucht 2000). This occurs in cases where there are not sufficient reflectance samples during a 16-day period to perform a full model inversion, in which case an archetypical BRDF shape is assumed based on a pre-existing land cover map of the region. This assumes that within a given cover type, BRDF shape will vary far less than magnitude. This has been shown to be a reasonable assumption given that BRDF shape is dominated by canopy structure (Knyazikhin *et al.* 2004). The number of full inversions over the Hill Farm during the period of available MODIS data is only five: none in 2000, 9 May and 13 August 2001 and 22 March, 7 April and 12 July 2002. This illustrates the difficulty of obtaining enough samples over the UK, even over a 16-day window, to invert any kind of BRDF model. This means that the majority of the parameters for the Barton Bendish site are in actual fact derived from a land cover map of the region. In this case, the parameters would be expected to show consistency by definition, as they are pre-determined and not based on observations.

3. Results and discussion

Figure 6 shows a comparison of broadband albedo measured using the CNR 1 net radiometer (7 May 2000 and 17 June 2000), broadband albedo derived from

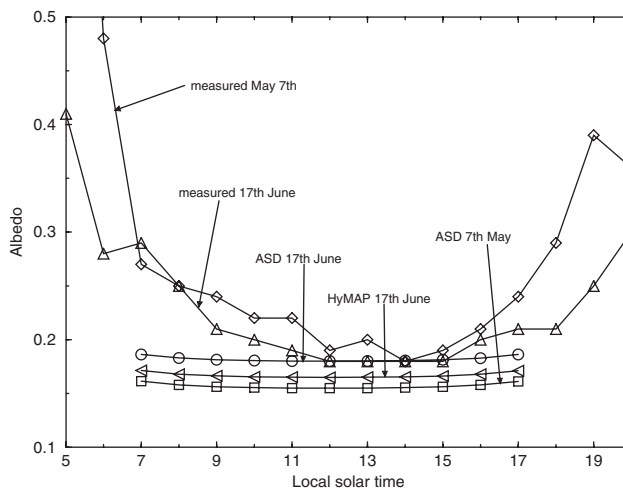


Figure 6. Comparison of broadband albedo measured using the CNR 1 net radiometer (labelled 'measured'), broadband albedo derived from reflectance measured using the ASD Fieldspec FR instrument (labelled 'ASD') and broadband albedo derived from the HyMAP agglomerated 'scene' wheat reflectance.

reflectance measured using the ASD Fieldspec Pro instrument (7 May 2000 and 17 June 2000) and broadband albedo derived from the HyMAP agglomerated 'scene' wheat reflectance values (17 June 2000). Variation in albedo is shown throughout the day. The HyMAP and ASD-derived albedo data are extrapolated over the day from the values calculated at the time of acquisition (near noon), weighted by varying solar irradiance throughout the day (the assumption is that the reflectance behaviour will not change significantly over a single day but the distribution of direct and diffuse illumination will).

Figure 6 shows that the broadband albedo values for wheat derived from the HyMAP and ASD measured reflectance data agree reasonably well both with each other and with the CNR 1 measured albedo values. The HyMAP and ASD-derived albedo are between 1% and 4% lower than those recorded using the CNR 1 net radiometer at noon. This is likely to be due to a slight discrepancy in the calculation of direct and diffuse illumination using the sky radiance model, as this is used to convert both HyMAP and ASD reflectances to albedo. The CNR 1 albedo values are based on measurements of incoming solar radiation. The standard mid-latitude summer atmospheric profile and continental aerosol model may not be the most appropriate but with no other information available there is no justification for choosing another combination. Measurements of aerosol optical depth and/or ozone and atmospheric water vapour made simultaneously with the ASD and HyMAP data would permit sky radiance to be calculated more accurately (a CIMEL sun photometer was in place during 1999 and 2000 for just this purpose but it was unfortunately not functioning correctly at the time of the other measurements).

The values of ASD-derived albedo (noon) for 17 June are around 4% higher than those for 7 May. This difference is not seen in the CNR 1 observations for the two dates, which are within 1% of each other. The expected rise in observed albedo at high solar zenith angles is far less pronounced for the ASD and HyMAP derived albedo than for the CNR 1 observations. This is due to the atmosphere being far more variable in practice than is assumed in the modelled sky radiance. However, the CNR 1 observations should be disregarded before 10:00 and after 17:00 as the atmospheric scattering is extreme at these times while the total insolation is actually at its lowest. The good agreement between the values of albedo measured using the CNR 1 instrument and those derived from ASD and HyMAP data (within 5% of each other) indicates that the albedo measurements made on the ground and those derived from the HyMAP data are consistent with each other, giving confidence in the measurements and in the assumptions that underpin them.

Figure 7 shows a comparison of the albedo values derived from all sources over Hill Farm, except the SPOT-VGT data from 1999. Albedo values for single dates comprise: CNR 1 measurements; those derived from the ASD measured reflectance spectra; those derived from HyMAP reflectance data (both individual fields and aggregate wheat reflectance); those derived from the Landsat TM scene for 11 July 1999. Time series of albedo comprise MOD43 albedo for the period 2000 to 2002.

It can be seen in figure 7 that there is reasonable agreement between the Landsat TM albedo and the MODIS data, with the Landsat TM value being between 2 and 4% higher than the MODIS values at the same time of year (11 July). Given that the Landsat TM scene is from 1999 while the MODIS data are from 2000–2002 respectively some small variability from year to year is not unexpected. The HyMAP wheat field and aggregated wheat albedo agree closely with both MODIS albedo values at the same time of year (17 June), as well as with the CNR 1

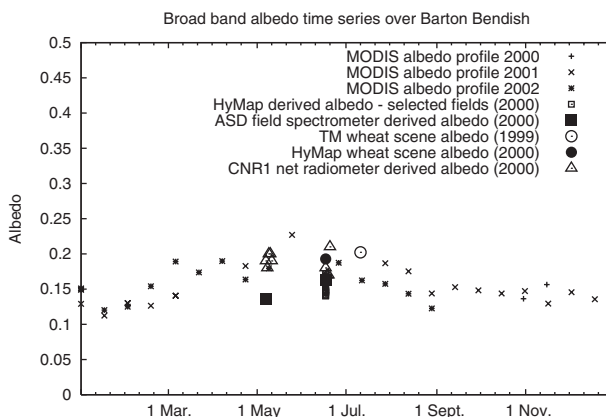


Figure 7. Comparison of albedo derived from the CNR 1 instrument (7 May 2000 and 17 June 2000), ASD measured reflectance data (7 May 2000 and 17 June 2000), HyMAP reflectance data (17 June 2000), Landsat TM data (11 July 1999) with time series of MOD43 albedo for the period 2000 to 2002.

measured values. The aggregated HyMAP wheat albedo values and the CNR 1 values lie between the MODIS values for 17 June 2001 and 2002. The ASD-derived values of albedo are only 1 or 2% lower. Earlier in the year (7 May) where there are CNR 1 measured and ASD-derived values of albedo (but no HyMAP or Landsat TM-derived values) there is still close agreement (<1%) between the CNR 1 measured values and the MODIS data. However the ASD-derived albedo values are some 6% lower than the CNR 1 and MODIS values here. This is likely to be a result of uncertainty in the ASD measurement due to unstable atmospheric conditions during measurement. The agreement between the various point-measured, field-measured, HyMAP, Landsat TM and MODIS values of albedo suggests that the values of albedo derived from MODIS data can be validated over the type of surface used in this study.

In addition to agreement between the MODIS albedo and the variety of other measurements of albedo, there is good temporal consistency between the time series of MODIS albedo. This is a result of magnitude inversion i.e. retrieval of BRDF parameters from the BRDF archetype database due to poor angular sampling. The temporal values of albedo from year to year between 2000 and 2002 agree very closely. The MODIS albedo values are compared with the SPOT-VGT albedo values in figures 9 and 10. The SPOT-VGT albedo values appear to fit in very closely to the MODIS temporal profiles.

Figure 8 shows the same comparison as presented in figure 7 (CNR 1, ASD, HyMAP, Landsat TM and MODIS albedo values), but this time for the four MODIS pixels immediately abutting the pixel centred on Hill Farm. The variation from the central pixel to the surrounding pixels is very small i.e. MODIS albedo values are consistent between the pixel used in figure 7 and the surrounding pixels. Consequently there is close agreement between the MODIS albedo values and the other sources of albedo as above. This supports the assertion that although the Hill Farm area is heterogeneous at the scale of the high resolution airborne and satellite data, it is largely homogeneous at the scale of the MODIS and SPOT-VGT data (note that uncertainty in the spatial registration of the SPOT-VGT data of up to 0.5 km will act to increase homogeneity). Although there is significant sub-pixel

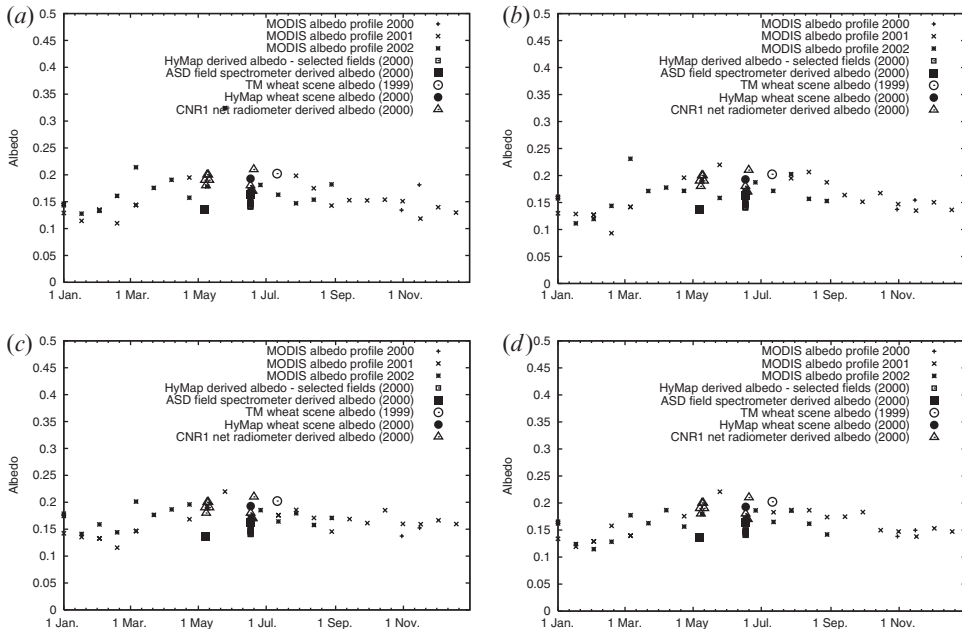


Figure 8. Comparison of albedo values as in figure 7 (CNR 1, ASD, HyMAP, Landsat TM and MODIS), for the four MODIS pixels immediately abutting the pixel centred on Hill Farm: (a) the pixel to the North; (b) the pixel to the West; (c) the pixel to the East; (d) the pixel to the South.

mixing of cover types, this mixing is relatively homogeneous across relatively large areas. This is a result of the area consisting almost exclusively of crops of similar reflectance and growth characteristics, in similar spatial mixtures.

Figures 9 and 10 show comparisons of the red (figure 9) and NIR (figure 10) black-sky (bs) albedo ($\bar{\rho}$) derived from SPOT-VGT data from May to October 1999 with MODIS data over the period October 2000 to October 2002. The temporal

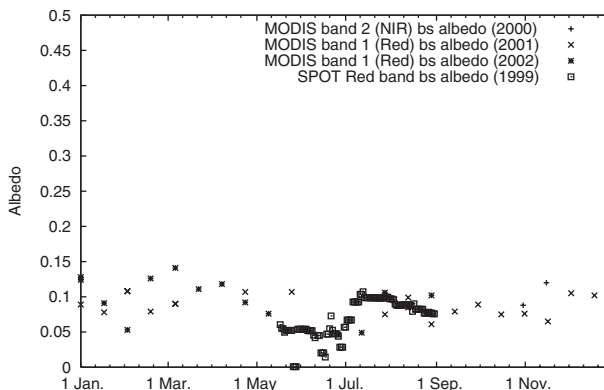


Figure 9. Comparison of the (broadband visible) red black-sky (bs) albedo ($\bar{\rho}$) derived from SPOT-VGT data from May to October 1999 with MODIS data over the period October 2000 to October 2002.

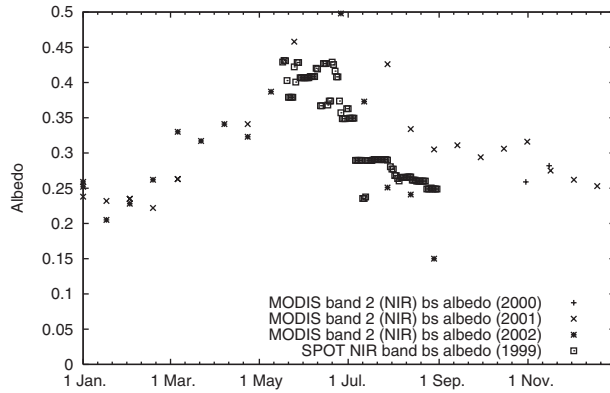


Figure 10. Comparison of the (broadband) NIR black-sky (bs) albedo ($\bar{\rho}$) derived from SPOT-VGT data from May to October 1999 with MODIS data over the period October 2000 to October 2002.

consistency between MODIS albedo values from one year to the next reflects the fact that more than 85% of the values are derived via magnitude inversions.

The MODIS data clearly pick up the reduction in albedo in the visible red due to the emergence and development of the main cereal crops (due to increasing photosynthetic activity) in the spring (mid-May), through to a rapid increase in July and August when harvesting occurs and bare soil is exposed once more. The SPOT-VGT data generally agree extremely closely with the MODIS albedo values in the visible red over the period May to October. The trends in visible red black-sky albedo noted above are followed very closely by the SPOT-VGT data, other than one or two outliers at the end of May 1999 when the SPOT-VGT albedo values are much lower than the corresponding MODIS values. Ignoring these anomalous values the SPOT-VGT albedo data appear to vary more smoothly than the MODIS data, because they are derived from data over 30 days rather than 16 days and are processed over a moving window, unlike the MODIS data which are processed in 16-day blocks.

Figure 10 shows the same time series comparison of SPOT-VGT and MODIS black-sky albedo but this time for the NIR region. The values are significantly higher than in the visible red case, ranging between 0.2 and 0.45 (as opposed to between 0.1 and 0.25 as in the red case). This is to be expected in an area dominated by vegetation over dark soils. The agreement between SPOT-VGT and MODIS albedo values is close, as in the May to September period (despite the different years). The NIR albedo values however are significantly more variable than was the case for the visible red. The rise in NIR albedo that would be expected to accompany the observed fall in visible red albedo during the 'greening up' of the region from mid-May to July is seen clearly in both SPOT-VGT and MODIS albedo values. The agreement between MODIS albedo values (predominantly derived via magnitude inversion) and SPOT-VGT albedo values (full inversion) suggests that the archetypical BRDF used within the magnitude inversions have been well chosen for this cover type.

4. Conclusions

A series of remote measurements of albedo over an agricultural site in the UK have been compared in order to provide a consistency check between albedo

measurements made at various scales and partial validation of the MOD43 BRDF/albedo product. The measurements were made at a wide range of spatial scales, from point measurements within individual wheat fields, to albedo values derived from moderate resolution satellite data (1 km). Ground-based measurements of albedo and albedo derived from ground-measured reflectance were scaled up to moderate resolution satellite-derived values of albedo (1 km) through values of albedo calculated from airborne and satellite data at high resolution (4 m and 30 m respectively). It has been shown that the values derived at the various scales agree very well in absolute terms, although only single date measurements can be compared in the case of the airborne and high resolution satellite data. In the latter case, the data are from a previous year of the MODIS observations, although the region, cover type and land use are known to be consistent from year to year during this period.

A major difficulty in utilizing albedo derived from optical remote sensing data over a region such as the UK is that multiple angular samples of surface reflectance are required in order to invert BRDF models against reflectance data. Even for a product such as MOD43 BRDF/albedo which is derived over a 16-day window as a compromise between achieving sufficient angular sampling whilst still capturing vegetation dynamics, it was seen that only five full inversions were possible over the field site during the entire 24 month period of MODIS data analysed, as a result of cloud cover.

The temporal variation of the MODIS albedo was internally consistent from year to year as would be expected by definition given that most values are derived from magnitude inversion. The MOD43 albedo values agree very well with those derived from the SPOT-VGT sensor, which has slightly different orbital characteristics, spectral bands and processing. The inter-annual variation of albedo values also agree well between SPOT-VGT and MODIS, with the rise and fall of albedo in the visible red and NIR following each other closely as well as conforming to expectations. This agreement suggests the albedo is actually relatively stable in this region and that if the remotely sensed data are processed carefully (in particular applying good cloud detection, accurate geometric registration and atmospheric correction techniques) then values can be compared from one sensor to another and from one year to another. The availability of long-term albedo data from MODIS allows comparison of production-level albedo over a significant length of time (inter-year and/or between sensors). Previous long-term datasets from which albedo may be derived (e.g. AVHRR) have suffered from instrument calibration, atmospheric and geometric correction and cloud contamination issues (Cihlar *et al.* 1994).

The good agreement between the MODIS and SPOT-VGT derived albedo values is an indirect validation of the magnitude inversion method used in the MOD43 product when too few angular samples are available for full model inversion (Strugnell and Lucht 2000). The values derived from SPOT-VGT are derived from observed reflectance and these values agree well both in magnitude and in temporal variability with those derived from MODIS via magnitude inversion.

It has been established that because broadband albedo is not an intrinsic surface property it can be difficult to validate (Liang *et al.* 2003). Validation requires that either measurements of atmospheric state (optical depth, and/or water vapour and ozone) be made simultaneously with any measurement of reflectance or albedo, or that assumptions be made about atmospheric scattering. In addition the number of

measurements that are required make it time-consuming and intensive (in particular, characterizing variability from a range of sources). Further, albedo at the scale of the MOD43 BRDF/albedo product (1 km) scale is difficult to validate: either measurements are required over extremely homogeneous surfaces (e.g. desert) (Liang *et al.* 2003); or, as in this study, measurements over a range of scales and assumptions about spatial heterogeneity must be made. It has been shown that measurements of albedo made at point and field scales can be scaled up through high resolution airborne and satellite data to moderate resolutions. In this case it is required that any inconsistencies between each resolution be quantified and/or understood. Ideally it would be possible to conduct validation measurements over the entire growing season for multiple years in order to quantify changes from year to year, but acquiring field data and high resolution EO data (especially airborne) is both expensive and very difficult over the UK where cloud cover can be restrictive. As a result, comparisons must be made using the measurements that are available.

In this study, the wheat fields in which point measurements of albedo and reflectance were made were assumed to be Lambertian. This was to allow directional hemispherical reflectance (and hence albedo) to be calculated despite having too few angular samples of reflectance to invert a model of BRDF as would ideally be the case. This was shown to be a reasonable assumption given the lack of angular variability observed in either the ground-measured or airborne HyMAP reflectance. The Lambertian assumption was extended to the Landsat TM data. To generate albedo from the various field-measured, HyMAP and Landsat TM reflectance data assumptions regarding the atmospheric state were also required. This is perhaps the greatest uncertainty in the scaling-up process. A sky radiance model was used to calculate the direct and diffuse components of illumination and the fact that albedo derived from the field-measured, HyMAP and Landsat TM data were slightly lower than those measured directly using the CNR 1 net radiometer suggest that the sky radiance distribution may not be quite correct. However, with no information on atmospheric state available there is no justification for changing the values of the sky radiance model parameters.

It is clear that despite the difficulties of validating broadband albedo, it can be done given a range of data and at various scales and making a few assumptions. The MOD43 BRDF/albedo product (albeit derived largely from magnitude inversions) has been shown to agree closely in temporal profile with albedo values derived from SPOT-VGT moderate resolution data. This in itself provides confidence in the magnitude inversion method employed in deriving the MOD43 BRDF/albedo product when too few angular samples are available for a full BRDF model inversion, such as is likely over the UK and other cloudy regions.

Acknowledgments

This work was partially funded under various UK Natural Environment Research Council (NERC) research and training grants (award GR3/1169), the NERC Centre for Terrestrial Carbon Dynamics (CTCD) and ESA contract AO/1-3679/00/NL/NB. The ASD Fieldspec FR radiometer was provided by the NERC Equipment Pool for Field Spectroscopy (EPFS). Many thanks to Mr Brian Reynolds for his permission for access to Hill Farm and support for our work and to Jo Shaw and Paul Hobson for access to field measurements. Thanks are also due to the MODIS BRDF/albedo team at Boston University, USA and NASA and the MODLAND team for their kind assistance.

References

- BOARDMAN, J., 1998, Post-ATREM polishing of AVIRIS apparent reflectance data using EFFORT: a lesson in accuracy versus precision. *Summaries of the Seventh JPL Airborne Earth Science Workshop*, 13 January, Pasadena CA, JPL Publication 97-21, 1, p. 53.
- BREST, C. L., and GOWARD, S. N., 1987, Deriving surface albedo measurements from narrow band satellite data. *International Journal of Remote Sensing*, **8**, 351–367.
- CIHLAR, J., MANAK, D., and VOISIN, N., 1994, AVHRR bidirectional reflectance effects and compositing. *Remote Sensing of Environment*, **48**, 77–88.
- DICKINSON, R. E., PINTY, B., and VERSTRAETE, M. M., 1990, Relating surface albedos in GCMs to remotely sensed data. *Agricultural Forest Meteorology*, **52**, 109–131.
- DISNEY, M. I., 2002, Improved estimation of surface biophysical parameters through inversion of linear BRDF models. PhD thesis, University of London, UK (available from the author).
- DISNEY, M. I., MULLER, J.-P., LEWIS, P., and BARNSLEY, M. J., 1997, Production and validation of BRDF and albedo extracted from airborne and spaceborne data. *Proceedings of the 7th International Symposium on Physical Measurements and Signatures in Remote Sensing, Courchevel, France, 7–11 April 1997*, vol. 2 (Rotterdam, The Netherlands: A. A. Balkema), pp. 471–478.
- GAO, B.-C., HEIDEBRECHT, K. B., and GOETZ, A. F. H., 1996, *Atmospheric Retrieval Program (ATREM) Version 2.0 Users Guide* (Boulder, CO: Center for the Study of Earth from Space/CIRES).
- KNYAZIKHIN, Y., MARSHAK, A. L., and MYNENI, R. B., 2004, Three-dimensional radiative transfer in vegetation canopies. In *Three-Dimensional Radiative Transfer in the Cloudy Atmosphere*, edited by A. Davis and A. Marshak (New York: Springer-Verlag) (forthcoming).
- LEWIS, P., DISNEY, M. I., BARNSLEY, M. J., and MULLER, J.-P., 1999, Deriving albedo maps for HAPEX-Sahel from ASAS data using kernel-driven BRDF models. *Hydrology and Earth System Science*, **3**, 1–13.
- LIANG, S., 2000, Narrowband to broadband conversions of land surface albedo: I Algorithms. *Remote Sensing of Environment*, **76**, 213–238.
- LIANG, S., and LEWIS, P., 1996, A parametric radiative transfer model for sky radiance distribution. *Journal of Quantitative Spectroscopy and Radiative Transfer*, **55**, 181–189.
- LIANG, S., FANG, H., CHEN, M., SHUEY, C. J., WALTHALL, C., DAUGHTRY, C., MORISSETTE, J., SCHAAP, C., and STRAHLER, A. H., 2002, Validating MODIS land surface and albedo products: methods and preliminary results. *Remote Sensing of Environment*, **83**, 149–162.
- LIANG, S. L., SHUEY, C. J., RUSS, A. L., FANG, H. L., CHEN, M. Z., WALTHALL, C. L., DAUGHTRY, C., and HUNT, R., 2003, Narrowband to broadband conversions of land surface albedo: II. Validation. *Remote Sensing of Environment*, **84**, 25–41.
- LUCHT, W., SCHAAP, C. B., and STRAHLER, A. H., 1999, An algorithm for the retrieval of albedo from space using semiempirical BRDF models. *IEEE Transactions on Geoscience and Remote Sensing*, **38**, 977–998.
- LUCHT, W., HYMAN, A. H., STRAHLER, A. H., BARNSLEY, M. J., HOBSON, P., and MULLER, J.-P., 2000, A comparison of satellite-derived spectral albedos to ground-based broadband albedo measurements modeled to satellite spatial scale for a semidesert landscape. *Remote Sensing of Environment*, **74**, 85–98.
- MARTONCHIK, J. V., DINER, D. J., PINTY, B., VERSTRAETE, M. M., MYNENI, R. B., KNYAZIKHIN, Y., and GORDON, H. R., 1998, Determination of land and ocean reflective, radiative and biophysical properties using multiangle imaging. *IEEE Transactions on Geoscience and Remote Sensing*, **36**, 1266–1281.
- MORISSETTE, J. T., PRIVETTE, J. L., and JUSTICE, C. O., 2002, A framework for the validation of MODIS Land products. *Remote Sensing of Environment*, **83**, 77–96.
- NICODEMUS, F. E., RICHMOND, J. C., HSIA, J. J., GINSBURG, I. W., and LIMPERIS, T., 1977, Geometrical consideration and nomenclature for reflectance. National Bureau of Standards Report, NBS MN-160, Washington, DC, 52 pp.
- PASSOT, X., 2000, VEGETATION image processing methods in the CTIV. *Proceedings of VEGETATION 2000: Two years to prepare for the future, Italy, April 2000* (European Commission), pp. 15–22.

- RAHMAN, H., and DEDIEU, G., 1994, SMAC: a simplified method for atmospheric correction of satellite measurements in the solar spectrum. *International Journal of Remote Sensing*, **15**, 123–143.
- SAICH, P., LEWIS, P., DISNEY, M., and THACKRAH, G., 2001, Comparison of Hymap/E-SAR data with models for optical reflectance and microwave scattering from vegetation canopies. *Proceedings of the Third International Workshop on Retrieval of Bio- and Geo-Physical Parameters from SAR Data for Land Applications, Sheffield, September 2001* (ESA Publication SP-475), pp. 75–80.
- SCHAAF, C. B., GAO, F., STRAHLER, A. H., LUCHT, W., LI, X., ZHANG, X., JIN, Y., TSVETSINSKAYA, E., MULLER, J.-P., LEWIS, P., BARNESLEY, M., ROBERTS, G., DISNEY, M., DOLL, C., LIANG, S., ROY, D., and PRIVETTE, J., 2001, Land surface albedo, nadir BRDF-adjusted reflectance and BRDF product from the Moderate Resolution Imaging Spectroradiometer (MODIS). *Proceedings of the 11th Conference on Satellite Meteorology and Oceanography, AMS, Madison, WI, 15–18 October 2001* (Lawrence, KS: Allen Press), pp. 5–21.
- SCHAAF, C., STRAHLER, A., LUCHT, W., TSANG, T., GAO, F., LI, X., STRUGNELL, N., CHEN, L., MULLER, J.-P., LEWIS, P., BARNESLEY, M. J., HOBSON, P., DISNEY, M. I., DUNDERDALE, M., D'ENTREMONT, R. P., HU, B., and LIANG, S., 2002, The At-launch MODIS BRDF and Albedo Science Data Product. *Remote Sensing of Environment*, **83**, 135–148.
- SELLERS, P. J., 1992, Remote sensing of the land surface for studies of global change, NASA/GSFC. International Satellite Land Surface Climatology Project Report, Greenbelt, MD, USA.
- SELLERS, P. J., 1995, Biophysical models of land surface processes. In *Climate System Modelling*, edited by K. E. Trenberth (Cambridge: Cambridge University Press), pp. 451–490.
- SHAW, J., 2002, Use of plant growth simulations to validate BRDF model parameters derived from SPOT-VGT data. PhD thesis, University of Wales Swansea, UK.
- SONG, J., and GAO, W., 1999, An improved method to derive surface albedo from narrowband AVHRR satellite data: narrowband to broadband conversion. *Journal of Applied Meteorology*, **38**, 239–249.
- STRAHLER, A. H., MULLER, J.-P., LUCHT, W., BARKER SCHAAF, C., TSANG, T., GAO, F., LI, X., LEWIS, P., BARNESLEY, M., STRUGNELL, N., HU, B., HYMAN, A., D'ENTREMONT, R. P., CHEN, L., LIU, Y., MCIVER, D., LIANG, S., DISNEY, M., HOBSON, P., DUNDERDALE, M., and ROBERTS, G., 1999, MODIS Product ID: MOD43 MODIS BRDF/Albedo Product: Algorithm Theoretical Basis Document Version 5.0. NASA GSFC, Greenbelt, MD, USA.
- STRUGNELL, N. C., and LUCHT, W., 2000, An algorithm to infer continental-scale albedo from AVHRR data, land cover class, and field observations of typical BRDFs. *Journal of Climate*, **14**, 1360–1376.
- SYLVANDER, S., HENRY, P., BASTIN-THIRY, C., MEUNIER, F., and FUSTER, D., 2000, VEGETATION geometrical image quality. *Proceedings of VEGETATION 2000: Two years to prepare for the future, Italy, April 2000* (European Commission).
- VERMOTE, E. F., TANRÉ, D., DEUZÉ, J. L., HERMAN, M., and MORCRETTE, J. J., 1997, Second simulation of the satellite signal in the solar spectrum (6S): an overview. *IEEE Transactions on Geoscience and Remote Sensing*, **35**, 675–686.
- WANNER, W., STRAHLER, A. H., HU, B., LEWIS, P., MULLER, J.-P., LI, X., BARKER SCHAAF, C. L., and BARNESLEY, M. J., 1997, Global retrieval of bidirectional reflectance and albedo over land from EOS MODIS and MISR data: theory and algorithm. *Journal of Geophysical Research*, **102**, 17143–17161.
- ZIBORDI, G., and VOSS, K. J., 1989, Geometrical and spectral sky radiance: comparison between simulations and field measurements. *Remote Sensing of Environment*, **27**, 343–358.